Penerbit Akademia Baru

Journal of Advanced Research in Materials Science
ISSN (online): 2289-7992 | Vol. 12, No.1. Pages 1-11, 2015

Studies on Thermal and Conductivity of Modified Natural Rubber

S. N. H. Mohd Yusoff [*,1], *L. H. Sim*[2], *C. H. Chan*[3], *S. S. Sheikh Abdul Aziz*[4], *Z. S. Mahmud*[4], *and H. Mohd Hairi*[1]

[1]Faculty of Applied Sciences, Universiti Teknologi MARA, Cawangan Johor Kampus Pasir Gudang, Jalan Purnama, Bandar Seri Alam, 81750 Masai, Johor, Malaysia.
[2]Centre of Foundation Studies, Universiti Teknologi MARA, 42300 Puncak Alam, Selangor, Malaysia.
[3]Faculty of Applied Sciences, Universiti Teknologi MARA, 40450 Shah Alam, Selangor, Malaysia.
[4]Faculty of Applied Sciences, Universiti Teknologi MARA, Cawangan Perak Kampus Tapah, 35400 Tapah Road, Perak, Malaysia.
[*]*sitinorhafiza@johor.uitm.edu.my*

Abstract – *Epoxidized natural rubber (ENR) and methyl-grafted natural rubber (MG) were chosen as a polymer host in this study with introduce of Li-salt by using solution casting technique. Values of glass transition temperature (T_g) obtained using differential scanning calorimetry (DSC) and the ionic conductivity evaluated from bulk resistance (R_b) determined using the impedance spectroscopy point towards the higher solubility of the lithium salt in MG rubber. Dependency of dielectric constants (ε') on salt concentration is more pronounced at low frequencies from 50 Hz to approximately 1.0 x 104 Hz. Ionic conductivities (σ) as well as the dielectric constants (ε') are observed to increase with ascending salt content for all systems. Meanwhile, two T_gs was observed in MG-rubber systems shows that the efficiency of the grafting is weak and can be confirm with spectroscopic results demonstrated in FTIR spectra.*

Keywords: Polymer Electrolytes, Conductivity, Glass Transition Temperature (T_g), Rubber

1.0 INTRODUCTION

Solid polymer electrolytes (SPE) are ion conducting, solvent-free polymer films composes of alkali salts dissolved in a polymer matrix. From the past two decades till now, development of SPE continues to attract great research interest in the hope of opening new scenarios for enhanced electrical energy-storage and energy-generation devices. The discovery of ion conducting polymer in the seventies and its application as electrolyte in solid-state rechargeable lithium battery had created a conceptual revolution in the electrochemical industry [1]. The most frequently studied polymer in that context is poly(ethylene oxide) (PEO) due to its low glass transition temperature (T_g) and high solvating power for a wide variety of salts [2-9]. The presence of the lone pair electrons at the ether oxygen of PEO enables it to complex with high concentration of many types of salt [8,10,11]. It is widely acknowledged that the amorphous fraction of SPE plays a determinant role in ion transport processes, thus, lithium salts are

Journal of Advanced Research in Materials Science
ISSN (online): 2289-7992 | Vol. 12, No.1. Pages 1-11, 2015

expected to be molecularly dispersed in the amorphous regions of the host matrix. Undoped and doped-PEO demonstrate relatively low conductivity at ~10^{-10} and ~10^{-6} S cm^{-1} at room temperature, respectively [12].

Elastomers are macromolecular materials which can rapidly return to their approximate shape from which they have been substantially distorted by a weak stress [13]. Natural rubber (NR) and other modified NRs are examples of elastomer. Modification of NR aims at improving its properties and characteristics. As a result, certain modified NRs (MNR) possess low T_g, good mechanical properties and moderate ionic conductivity. Among these modifications, epoxidation has special significance, as it combines several important properties such as oil resistance, low air permeability, ionic conductivity and improved damping.

In this study, modified NRs such as epoxidized natural rubber (ENR) and poly(methyl methacrylate) (PMMA)-grafted NR (MG) have been used as the polymer host for the solid polymer electrolytes (SPE). Natural rubber with 25 mol% and 50 mol% of epoxidation, ENR-25 and ENR-50 and 30 wt% and 49 wt% of PMMA-grafted NR, MG-30 and MG-49 are the polymers of this study. The interesting attributes of the MNR are low T_g, soft elastomer characterization at room temperature, good elasticity and ionic conductivity. MNR with an optimal amount of elasticity forms a smooth, thin, and flexible film which gives excellent contact between an electrolytic layer and an electrode in any battery system. Furthermore, it can act as a polymeric solvent with higher ionic conductivity compared to the glassy or crystalline state of semi-crystalline polymer. Conductivity of the ENR and MG rubber is attributed to the presence of the oxygen atom in the oxirane and carboxyl group, respectively. The oxygen atoms with lone pair of electrons coordinate with Li^+ ions from the perchlorate salt forming a polymer-salt complex. To both ENR and MG-rubber, the coordination of Li^+ ion and oxygen atoms transform electrical insulating material into electrical conductor. However, interchain interactions at the polar epoxy and carbonyl group of the macromolecules, respectively, may lead to a reduction in segmental flexibility.

2.0 MATERIALS AND METHODS

Materials

Epoxidized natural rubber, ENR-25 and ENR-50 purchased from Malaysian Rubber Research Institute (Sungai Buloh, Malaysia) and deproteinized natural rubber (DPNR) and methyl-grafted natural rubber, MG-30 and MG-49 are gift from Green HPSP (M) Sdn. Bhd. were used after mastication. $LiClO_4$ was purchased from Across Organic Company (Geel, Belgium) and the solvent tetrahydrofuran (THF) was purchased from Merck.

Methods

Solution casting technique was used to prepare the solid polymer electrolytes of ENR and MG-rubber. Appropriate amount of the rubber and $LiClO_4$ were dissolved in THF by stirring with a magnetic stirrer at 50 °C until a homogeneous solution was obtained. The $LiClO_4$ content (Y) added varied in a range from 2-30 wt. % of the dry weigh of the polymer. It can be represented by Equation (1)

$$Y = \frac{\text{mass of salt}}{\text{mass of polymer}} \times 100\% \quad (1)$$

The electrolyte solution was cast into a Teflon dish and left to dry overnight at room temperature to form a thin film. The electrolyte films were dried in an oven for 24 hours at 50 °C before heating for another 24 hours in nitrogen gas atmosphere at 80 °C. This is to ensure a good interaction between the salt and the elastomer. The free standing film was further dried in a vacuum oven at 50 °C for another 24 hours before keeping in desiccators for further characterization.

Ionic Conductivity Measurements

The impedance measurements were measured using the HIOKI 3532-50 LCR Hi-Tester interfaced to a computer. The samples were scanned at frequencies ranging from 50 Hz to 1 MHz at room temperature. The thin film samples were crammed between two stainless steel block electrodes of 20 mm in diameter. The conductivity, σ, of each sample was calculated using the equation $\sigma = t/(R_bA)$, where t is the thickness of the sample, R_b is the bulk resistance and A is the cross-sectional area of the film. The R_b value is the intersection point between the semicircle and the x-axis in a cole-cole plot. The average of the thickness, t was calculated from four measurements of the thickness of the thin film by using Mitutoyo Digimatic Caliper (Japan).

Differential Scanning Calorimetry

TA Q200 DSC which is calibrated with indium standard was used to obtain the thermal properties of the sample. For valuation of the glass transition temperature, T_g, approximately 10 - 12 mg of the sample was used for each analysis. The sample was cooled down to -90 °C and was heated up to 80 °C at a rate of 10 °C min^{-1}.

ATR-FTIR

Infrared spectra of all samples were obtained using ATR-FTIR Perkin Elmer at room temperature with frequency range of 4000 - 650 cm^{-1}. 32 scans were collected at resolution of 2 cm^{-1} using the Ge crystal plate for each sample.

3.0 RESULTS

Glass Transition Temperature

The glass transition temperature, T_g of a polymer observed as an endothermic shift from the specified baseline of a thermogram is determined using DSC. It is governed mainly by the heating and cooling rates used in the DSC run. The T_g values of the modified natural rubber (MNR), extracted from the second heating runs were presented in Fig. 1.

As shown in Fig. 1, ENR-50 with higher epoxidation level exhibits a more significant increase in T_g than ENR-25. Therefore, the oxirane group in ENR is the predominant coordination site between Li^+ and the ENRs. Higher T_g values in ENR-50 with concentration of salt (Y) ranged from 0.01 to 0.30 imply that the elastomer is stiffer and less elastomeric as compared to ENR-25 with the same salt concentration.

Penerbit Akademia Baru

Journal of Advanced Research in Materials Science
ISSN (online): 2289-7992 | Vol. 12, No.1. Pages 1-11, 2015

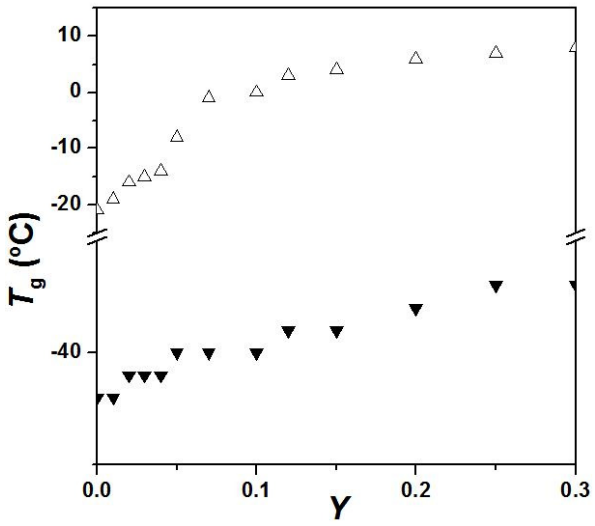

Figure 1: Glass Transition Temperatures of ENR; (▼) ENR-25, (Δ) ENR-50 with Different Concentration of Salt

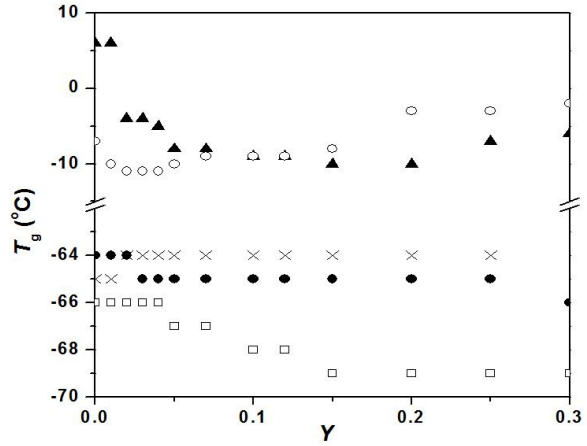

Figure 2: Glass Transition Temperatures of (×) DPNR, (●)(▲) MG-30, and (□)(○) MG-49 with Different Concentration of Salt

Figure 2 shows that the T_g values for DPNR remain relatively constant with increasing salt content which is about -65 to -64 °C. This is due to the extremely weak interaction between Li^+ ions and the π electrons of the C=C in the polymer chain of DPNR. Two T_gs are observed for both the MG rubbers (MG-30 and MG-49). The lower T_g value is attributed to the natural rubber segment of the MG-grafted copolymer because it is very close to the T_g value of DPNR while the higher T_g value is corresponding to the PMMA segment of the grafted copolymer. Incorporation of $LiClO_4$ does not increase the lower T_gs of both MG30 and MG49; instead, the T_gs decrease slightly. On the other hand, with ascending salt concentration, the T_g value corresponding to the PMMA segment of the copolymer, MG-30 decreases initially until Y = 0.20, then increases with higher salt content. Meanwhile, MG-49 shows the same behavior except that the T_g value increases at a much lower salt content at W_{salt} = 0.04.

Penerbit Akademia Baru

Journal of Advanced Research in Materials Science
ISSN (online): 2289-7992 | Vol. 12, No.1. Pages 1-11, 2015

Ionic Conductivity

Ionic conductivity for ENR-25, ENR-50 and DPNR evaluated at different concentrations of Li-salt at room temperature are presented in Fig. 3.

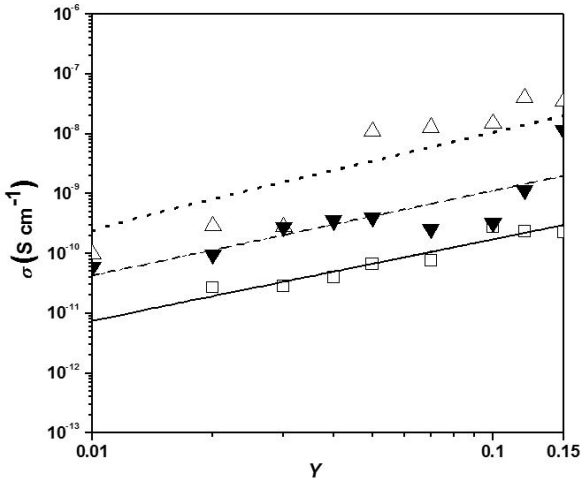

Figure 3: Quantities σ_{DC} versus Y of MNR Polymer Electrolytes at 30 ^{0}C. (□) DPNR, (▼) ENR-25, (Δ) ENR-50 with Dotted, Solid and Dashed Curves, respectively, Represents Linear Regression after Equation (2)

The ionic conductivity of both ENR-25 and ENR-50 increase with ascending salt content due to an increase in the number of charge carriers. Being a non-crystalline elastomer, the segmental motion of the macromolecular chain promote ion transport of lithium ions within the polymer [14]. As As mention in the discussion on T_g, the flexibility and the segmental motion of the polymer chain decreases with increasing epoxidation level and salt concentration. Therefore, the ionic conductivity of ENR-50 is observed to be lower than that of ENR-25 at the same salt concentration. A decline in the ionic conductivity for ENR-25 system is observed when the salt concentration, $Y > 0.15$ which is attributed to the increasing stiffness of the macromolecular chain which restricts ion transport within the polymer host [15]. At all salt concentration, the ionic conductivity of the solid solution of ENR-25 is the highest, about one order in magnitude higher than ENR-50 and two orders in magnitude than DPNR. Therefore, the enhanced conductivity of ENR-25 as compared to ENR-50 and DPNR is attributed to the presence of an optional number of epoxide groups which act as coordination sites for Li^+ ions while maintaining the good elastomeric characteristics of natural rubber.

At low salt concentration, the dependence of conductivity on $LiClO_4$ concentration, Y, can be described using the power law as shown in Equation (2).

$$\sigma_{DC} = N_A e(\alpha\mu)\frac{\rho_{MNR}}{M_{salt}}(Y)^x \quad (2)$$

where N_A represents Avogadro number, e is elementary charge, μ is ion mobility, α is degree of dissociation. Quantities μ and α are also functions of salt concentration. All concentration dependencies of conductivity are studied by a power law dependence of Y. Exponent x which are determined experimentally gives the extent of correlations between salt molecules and

Penerbit Akademia Baru

Journal of Advanced Research in Materials Science
ISSN (online): 2289-7992 | Vol. 12, No.1. Pages 1-11, 2015

MNR segments. Quantities μ and α are independent of concentration. Meanwhile, ρ_{MNR} and M_{salt} represent density of the MNR and molar mass of the salt molecule, respectively.

A double logarithmic plot of σ_{DC} versus Y gives the values of exponent x and the product of degree of dissociation and mobility ($\alpha\mu$) as shown in Figure 3. The regression functions after Equation (2) in Figure 3 are in Table 1. Molecular characteristics adopted for determination of quantity $\alpha\mu$ are M_{salt} (M_{LiClO4} : 106.5 g mol^{-1}), M_{MNR} (M_{DPNR} : 136 g mol^{-1} ; M_{ENR-25} : 144 g mol^{-1}; M_{ENR-50} : 152 g mol^{-1}) and ρ_{MNR} (ρ_{DPNR} : 0.920 g cm^{-3}; ρ_{ENR-25} : 0.971 g cm^{-3}; ρ_{ENR-50} : 1.027 g cm^{-3}). Adopting Nernst's relationship, one may relate the mobility $\alpha\mu$ to diffusion coefficient of the charge carriers. It follows

$$D = \frac{k_B T \alpha \mu}{e} \tag{3}$$

where k_B is the Boltzmann constant (k_B ; 1.381 x 10^{-23} m^2 kg s^{-2} K^{-1}) and T is the temperature in Kelvin at room temperature; 303 K.

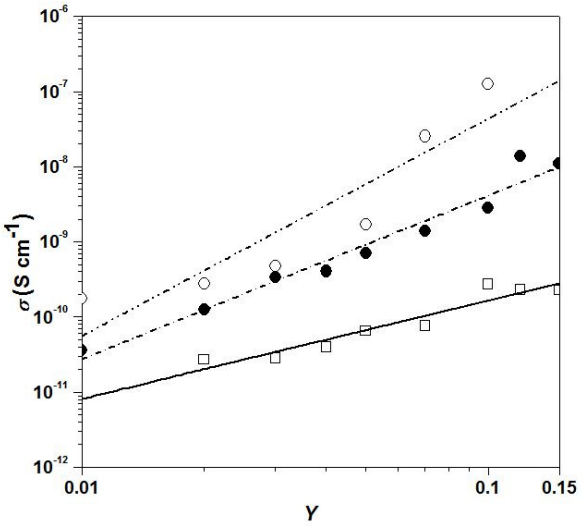

Figure 4: Quantities σ_{DC} versus Y for MNR Polymer Electrolytes at 30 ^{0}C. (□) DPNR, (●) MG-30 and (○) MG-49 with Dotted, Short Dashed-dotted and Dashed-dotted Curves, respectively, Represents Linear Regression after Eqn. (2)

Figure 4 illustrates the double log plot of σ_{DC} versus Y of MG-30, MG-49 and DPNR in the range of Y = 0.01 to 0.15. From the linear regression plot demonstrated in Figure 5, one can retrieved the values of the slope and the y-intercept. The values of $\alpha\mu$ and exponent x can then be evaluated following the example demonstrated for ENR-25.

All calculations of the regression function, ion mobility and diffusion function for all the MNR samples are shown in Table 1. Table 1 depicts that DPNR displays the lowest value of ion mobility ($\alpha\mu$), exponent x and diffusion coefficient (D) as compared to ENR and MG-rubber. This explains its lowest σ value among all the rubber samples and the weak interactions between the polymer segments and the salt molecules as discussed in the T_g section. In addition, it is noted that ENR-50 has a higher values of $\alpha\mu$, exponent x and D than ENR-25. This result correlates with the higher ionic conductivity of ENR-50 as compared to ENR-25 at low salt concentration range Y = 0.01 to 0.15. Meanwhile, the values of $\alpha\mu$ and D are two and one

Penerbit Akademia Baru

Journal of Advanced Research in Materials Science
ISSN (online): 2289-7992 | Vol. 12, No.1. Pages 1-11, 2015

order(s), respectively, higher for MG-49 than for MG-30. On the whole, among all the MNRs investigated in this work, MG-49 exhibits the highest ion mobility ($\alpha\mu$) of 3.6×10^{-8} cm^2 V^{-1} s^{-1}, the best correlation with the salt molecules (x = 2.89) and the highest diffusion coefficient (D) of 9.4×10^{-10} cm^2 s^{-1}.

Table 1: Regression Functions after Equation (2), Product Degree of Dissociation and Mobility ($\alpha\mu$); exponent x and Diffusion Coefficient (D) of MNR after Equation (3) for MNR with $LiClO_4$

	DPNR	ENR-25	ENR-50	MG-30	MG-49
Regression function	$\sigma_{DC} = 3.8 \cdot 10^{-9} Y^{1.35}$	$\sigma_{DC} = 2.9 \cdot 10^{-8} Y^{1.41}$	$\sigma_{DC} = 4.1 \cdot 10^{-7} Y^{1.58}$	$\sigma_{DC} = 6.2 \cdot 10^{-7} Y^{2.18}$	$\sigma_{DC} = 3.4 \cdot 10^{-5} Y^{2.89}$
Correlation, *R*	0.97	0.84	0.91	0.98	0.90
Exponent *x*	1.35	1.41	1.58	2.18	2.89
$\alpha\mu$ (cm^2 V^{-1} s^{-1})	$4.6 \cdot 10^{-12}$	$3.3 \cdot 10^{-11}$	$4.4 \cdot 10^{-10}$	$7.0 \cdot 10^{-10}$	$3.6 \cdot 10^{-8}$
D (cm^2 s^{-1})	$1.2 \cdot 10^{-13}$	$8.5 \cdot 10^{-13}$	$1.1 \cdot 10^{-11}$	$1.8 \cdot 10^{-11}$	$9.4 \cdot 10^{-10}$

ATR-FTIR

FTIR spectroscopic analysis was done using Attenuated Total Reflectance (ATR) method with Germanium crystal. The range of the spectra was recorded from 650 to 4000 cm^{-1} with the resolution 2 cm^{-1} and averaging 16 scans for all samples at room temperature. Figure 6 shows the spectra for the neat modified natural rubber of DPNR, ENR-25, ENR-50, MG-30 and MG-49. The characteristic absorption peaks for DPNR, ENR and MG-rubber are listed in Table 2.

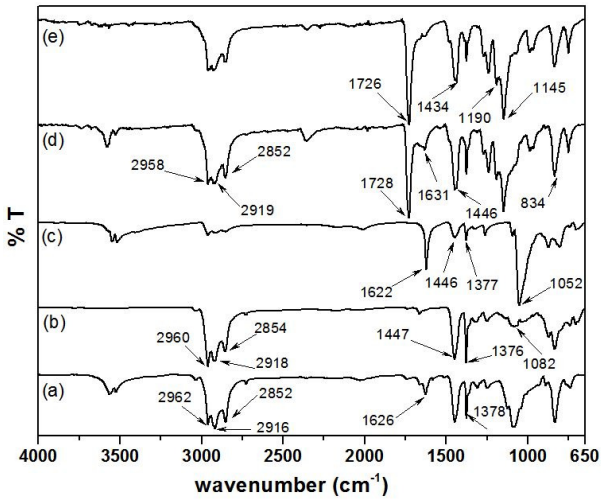

Figure 5: FTIR Spectra For Neat Polymer (a) DPNR, (b) ENR-25, (c) ENR-50, (d) MG-30, and (e) MG-49

The Li^+ ion from the $LiClO_4$ salt added to the MNR coordinates with the oxygen atoms of the polar groups of the MNR, thus, shifting the positions and/or changing the intensity of the absorption peaks of the polar groups concerned. To explore the interactions between the lithium ion and the various characteristic peaks of the rubber samples, the FTIR spectra of

Penerbit Akademia Baru

Journal of Advanced Research in Materials Science
ISSN (online): 2289-7992 | Vol. 12, No.1. Pages 1-11, 2015

DPNR/$LiClO_4$, ENR-25/$LiClO_4$, ENR-50/$LiClO_4$, MG-30/$LiClO_4$ and MG-49/$LiClO_4$ were analyzed.

Table 2: Wavenumber and Assignments of IR Band Exhibit by Neat ENR and MG-rubber.

Wavenumber (cm^{-1})	Assignment
2962, 2916, 2852	CH_2 stretching
1728	C=O stretching (corresponding to MG-rubber)
1626-1622	C=C stretching (corresponding to NR)
1445	CH_2 deformation modes
1378-1376	CH_2 wagging
1145 (MG-rubber), 1082-1052 (ENR)	C-O-C stretching mode
834	=C-H out-plane deformation

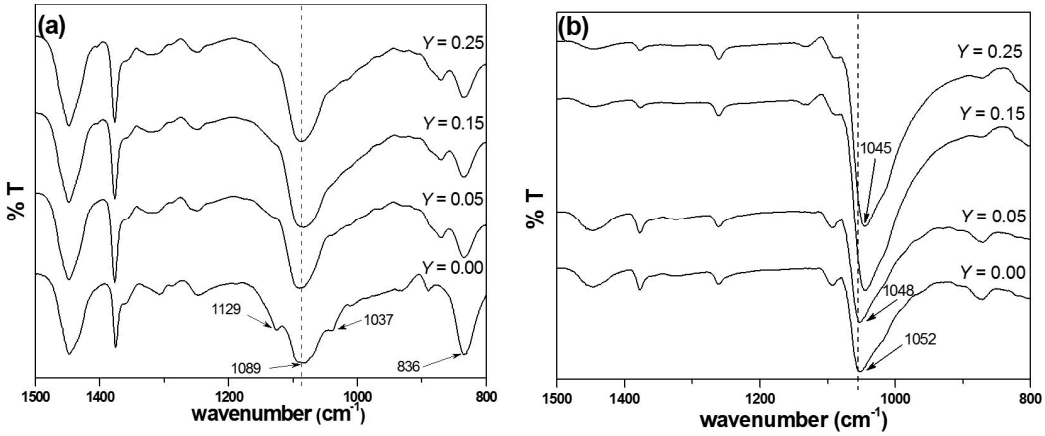

Figure 6: FTIR Spectra Showing the C-O-C Stretching in (a) ENR-25 and (b) ENR-50 with Different Values of *Y*

The triplet centered at 1089 cm^{-1} with two shoulders at 1037 and 1129 cm^{-1} as shown in Fig. 6(a) is assigned to the C-O-C stretching mode of the oxirane group in ENR-25. Addition of $LiClO_4$ from Y = 0 to 0.25 into ENR-25 results in the vanishing of the two shoulders, representing the coordination of Li^+ to the oxygen atom of the oxirane group. However, no significant shifting of the centre peak at 1089 cm^{-1} is observed. On the other hand, Figure 6(b) depicts that addition of the same amount of salt to ENR-50 causes C-O-C stretching mode which absorbs at 1052 cm^{-1} to downshift to 1048 cm^{-1} at Y = 0.05 and to 1045 cm^{-1} at higher salt concentration. The downshifting of the C-O-C vibrational mode observed in ENR-50 and not in ENR-25 implies that more lithium salt is coordinated to ENR-50 as compared to ENR-25. This result concurs closely with that observed in the T_g values discussed in the T_g section. Besides, the absorption peak at 836 - 834 cm^{-1} corresponding to the oxirane ring of both ENR-25 and ENR-50 as shown in Fig. 6 decreases in intensity when the salt content increases implying a decrease in the electron environment of the oxirane oxygen atom as it forms an ion-dipole interaction with Li^+ ion.

Penerbit Akademia Baru

Journal of Advanced Research in Materials Science
ISSN (online): 2289-7992 | Vol. 12, No.1. Pages 1-11, 2015

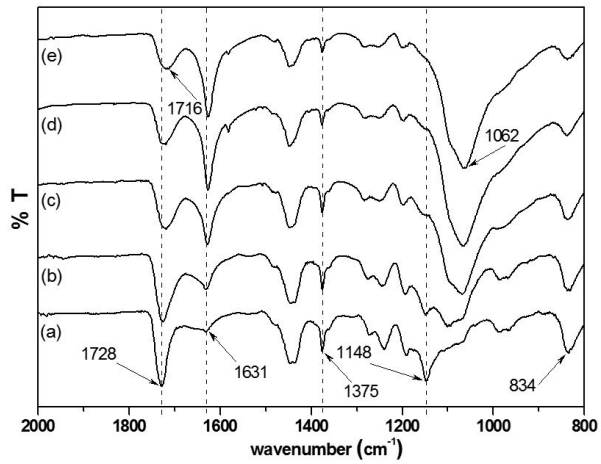

Figure 7: Spectra of MG-30 with (a) Neat, (b) $Y = 0.05$, (c) $Y = 0.10$, (d) $Y = 0.20$ and (e) $Y = 0.30$.

The characteristic peaks of the PMMA-grafted rubber are the carboxyl group, (COO^-). As shown in Fig. 7, the symmetric stretching peak of the carbonyl C=O bond which absorbs intensely at 1728 cm^{-1} is observed to reduce in intensity and downshifted from 1728 to 1716 cm^{-1} [16]. When Li^+ salt is added to the grafted copolymer, the shifting of the peak is caused by the coordination between Li^+ ion from the doping salt with the oxygen atoms of the C=O group. The peak at 1631 cm^{-1} assigned to the unsaturated C=C is observed to increase in intensity and form a sharp peak as the salt content increases. However, no significant shifting of the peak is observed. The asymmetric stretching of CH_2 at 1375 cm^{-1} gives a sharp peak and became weaker in intensity at $Y = 0.05$. Meanwhile, the C-O-C stretching mode of the carboxyl group which gives a medium peak at 1148 cm^{-1} downshifts to 1062 cm^{-1} with the addition of salt up to $Y = 0.30$.

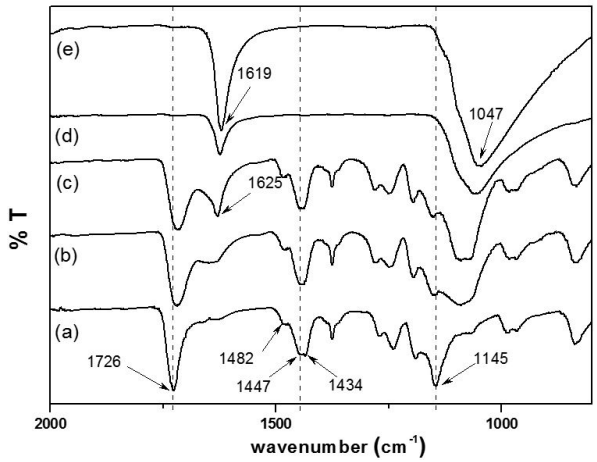

Figure 8: Spectra of MG-49 with (a) Neat, (b) $Y = 0.05$, (c) $Y = 0.12$, (d) $Y = 0.25$ and (e) $Y = 0.30$.

The ion-dipole interaction between lithium salt and the MG-49 was studied by FTIR as shown in Figure 8. On the addition of salt, the symmetric stretching mode of the carbonyl, C=O bond observed at 1726 cm^{-1} downshifts slightly and reduces in intensity. A new band at 1625-1619

cm^{-1} appears when $Y \geq 0.12$. Its intensity became stronger with increasing salt content. The C-O-C band broadens and downshifts from 1145 cm^{-1} to 1047 cm^{-1} suggests a strong interaction between the Li^+ ion and the oxygen atom of the C-O-C bond which also affects the electron environment of the neighboring ethylene groups. The CH_2 asymmetric band at 1447 cm^{-1} disappears when salt concentration $Y \geq 0.20$. From the spectra of both MG-30 and MG-49, it seems that the Li^+ prefers to coordinate with the oxygen atom of the C-O-C bond.

CONCLUSIONS

Solid polymer electrolytes of ENR-25/$LiClO_4$, ENR-50/$LiClO_4$, MG-30/$LiClO_4$, MG-49/$LiClO_4$ and DPNR/$LiClO_4$ with various concentrations of $LiClO_4$ were successfully prepared using solution casting technique. The effect of $LiClO_4$ on the conductivity, thermal and viscoelastic properties and polymer-salt interaction of ENR and MG rubber were investigated by AC Impedance Spectroscopy, Differential Scanning Calorimetry, Dynamic Mechanical Analysis and ATR-FTIR, respectively. The T_g values show that solubility and coordination of the ionic salt are higher in ENR-50 with more epoxy oxygen in the backbone of the macromolecular chain. In addition, the variation in the T_g values of ENR-50 with increasing salt content correlates with increase in the ion-dipole interaction observed in the FTIR spectra of ENR-50, thus, reaffirm the higher solubility of $LiClO_4$ in ENR-50 as compared to ENR-25. Meanwhile, two T_gs were observed in PMMA grafted rubber. The lower T_g value corresponds to the NR and the higher T_g value corresponds to the PMMA. Addition of salt raises the higher T_g values of the MG rubbers whereas the lower T_g values slightly decrease. The conductivity of MG rubber is about 4 orders in magnitude higher than the NR and one order higher than ENRs. In a nutshell, conductivity for all the rubber samples investigated in this study decreases in the order MG-49 > MG-30 > ENR-50 > ENR-25 > DPNR. Besides that, viscoelastic properties were successfully carried out by using dynamic mechanical properties (DMA) with frequency scan at room temperature. The NR becomes stiffer and tougher with incorporation of salt grafting of PMMA into the NR backbone.

REFERENCES

[1] D.E. Fenton, J.M. Parker, P.V. Wright, Complexes of alkali metal ions with poly(ethylene oxide). Polymer 14 (1973) 589-589.

[2] M.B. Armand, J.M. Chabagno, M. Duclot, Polyethers as solid electrolytes, Elsevier, Amsterdam 131-136, 1979.

[3] P.R. Sorensen, T. Jacobson, Electrochimica Acta 27 (1982) 1975.

[4] E.A. Rietman, M.L. Kaplan, R.J. Cava, Lithium ion-poly (ethylene oxide) complexes. I. Effect of anion on conductivity. Solid State Ionics 17 (1985) 67-73.

[5] S.L. Maunu, J.J. Lindberg, Structural and electrical studies on poly(ethylene oxide) complexed with inorganic salts. Polymer Bulletin 17 (1987) 545-549.

[6] J. Li, E.A. Mintz, I.M. Khan, Poly(ethylene oxide)/poly(2-vinylpyridine)/lithium perchlorate blends. New materials for solid polymer electrolytes. Chemistry of Materials 4 (1992) 1131-1134.

[7] J.R. Dygas, B. Misztal-Faraj, Z. Florjańczyk, F. Krok, M. Marzantowicz, E. Zygadło-Monikowska, Effects of inhomogeneity on ionic conductivity and relaxations in peo and peo–salt complexes. Solid State Ionics 157 (2003) 249-256.

[8] M. Jaipal Reddy, J. Siva Kumar, U.V. Subba Rao, P.P. Chu, Structural and ionic conductivity of peo blend peg solid polymer electrolyte. Solid State Ionics 177 (2006) 253-256.

[9] W.-S. Young, P.J. Brigandi, T.H. Epps, Crystallization induced lamellar to lamellar thermal transition in salt-containing block copolymer electrolytes. Macromolecules 41 (2008) 6276-6279.

[10] M.B. Armand, M.J. Duclot, P. Rigaud, Polymer solid electrolytes: Stability domain. Solid State Ionics 3–4 (1981) 429-430.

[11] Y. Zhao, R. Tao, T. Fujinami, Enhancement of ionic conductivity of peo-litfsi electrolyte upon incorporation of plasticizing lithium borate. Electrochimica Acta 51 (2006) 6451-6455.

[12] F.M. Gray, Solid polymer electrolytes, VCH, New York, (Chapter 4), 1991.

[13] W. Hoffman, Vulcanization and vulcanizing agents, Maclaren And Sons, 7 Grape Street, London, 3, 1967.

[14] Y.M.Z.A. Ali A M M, Bahron H, S.R.H. Y, Electrochemical studies on polymer electrolytes based on pmma-grafted natural rubber for lithium polymer battery. 12 (2006) 303.

[15] R.H.Y. Subban, A.K. Arof, S. Radhakrishna, Polymer batteries with chitosan electrolyte mixed with sodium perchlorate. Materials Science and Engineering: B 38 (1996) 156-160.

[16] M.S. Su'ait, A. Ahmad, H. Hamzah, M.Y.A. Rahman, Preparation and characterization of pmma–mg49–liclo$_4$ solid polymeric electrolyte. Journal of Physics D: Applied Physics 42 (2009) 055410.